Magnetic switching and phase competition in the multiferroic antiferromagnet $Mn_{1-x}Fe_xWO_4$

F. Ye,[1,*] Y. Ren,[2] J. A. Fernandez-Baca,[1,3] H. A. Mook,[1] J. W. Lynn,[4] R. P. Chaudhury,[5] Y.-Q. Wang,[5] B. Lorenz,[5] and C. W. Chu[5]

[1]*Neutron Scattering Science Division, Oak Ridge National Laboratory, Oak Ridge, Tennessee 37831-6393, USA*

[2]*X-ray Science Division, Argonne National Laboratory, Argonne, Illinois 60439, USA*

[3]*Department of Physics and Astronomy, The University of Tennessee, Knoxville, Tennessee 37996-1200, USA*

[4]*NIST Center for Neutron Research, Gaithersburg, Maryland 20899, USA*

[5]*Department of Physics and TCSUH, University of Houston, Houston, Texas 77204-5002, USA*

(Received 3 October 2008; published 3 November 2008)

Elastic neutron scattering is used to study the spin correlations in the multiferroic $Mn_{1-x}Fe_xWO_4$ with $x=0.035$, 0.05, and 0.10. The noncollinear incommensurate (ICM) magnetic structure associated with the ferroelectric (FE) phase in pure $MnWO_4$ is suppressed at $x=0.035$ and completely absent at $x=0.10$. The ICM spin order and FE phase can be restored by applying a magnetic field along the spin easy axis. The low-T commensurate magnetic structure extends in both H/T with increasing Fe concentration. The systematic evolution of the magnetic and electric properties indicates that the noncollinear ICM spin order results from competing magnetic interactions and its stabilization can be tuned by the internal (x) or external (magnetic-field) perturbations.

DOI: 10.1103/PhysRevB.78.193101 PACS number(s): 75.50.Ee, 61.05.F−, 75.30.Kz, 75.25.+z

Magnetoelectric multiferroic materials, which exhibit ferroelectric (FE) and magnetic orders simultaneously, have attracted great attention in recent years.[1–4] A number of multiferroic materials among transition-metal oxides have been discovered including $RMnO_3$,[5,6] $TbMn_2O_5$,[7] $Ni_3V_2O_8$,[8] $LuFeO_4$,[9] and $CuFeO_2$.[10] The ability to mutually control both the electric and magnetic properties, for example, to flop the electric polarization (P) via external magnetic field (H) (Ref. 5) or to reverse the magnetic helicity by electric field (E),[11] makes this family of functional materials promising candidates for future technological applications. One common feature of the multiferroic materials is the presence of long-wavelength magnetic structures with noncollinear spin configurations. Several microscopic or phenomenological mechanisms[12–14] have been proposed to explain the spontaneous polarization induced by inhomogeneous magnetic order M. Essentially, the nonlinear coupling between P and M becomes possible in frustrated systems with spiral or helical magnetic structure. The symmetry allowed term $PM\partial M$ gives rise to the electric polarization as soon as an appropriate magnetic order sets in.

In the long-sought control of electric properties by magnetic field, the wolframite structure $MnWO_4$ appears to be a unique magnetic material exhibiting the multiferroic behavior.[15–17] Unlike the rare-earth manganites where the stabilization of a spiral magnetic structure at the transition-metal ion site often involves the ordering of the rare-earth spins,[18] $MnWO_4$ is known to be a frustrated antiferromagnet (AF) with only one kind of magnetic ion. The Mn^{2+} spins ($S=5/2$) in the system undergo several magnetic transitions in zero field ($H=0$).[19] The low-temperature (T) magnetic structure (AF1, E type) is collinear and commensurate (CM) [Fig. 1(a)], with wave vector $\mathbf{k}=(\pm 1/4, 1/2, 1/2)$. At temperatures between 7 K (T_{N1}) and 12 K (T_{N2}), the magnetic structure evolves into an incommensurate (ICM) elliptical spiral configuration (AF2) accompanied by the spontaneous electric polarization along the crystalline b axis [Fig. 1(b)]. Between T_{N2} and T_{N3} ($\approx$13.5 K), $MnWO_4$ becomes collinear ICM and paraelectric (AF3). Recently, it was found that by doping Fe at the Mn site, the electric properties of $Mn_{1-x}Fe_xWO_4$ ($x\approx 0.10$) are considerably modified.[20] The FE phase observed in $MnWO_4$ at $H=0$ is completely suppressed but can be restored with moderate magnetic field. In addition, there appears to be transitions between low and high electric polarized states in field. Magnetic phase diagrams were proposed based on a mean-field approach[20] to account for the observed interplay between the magnetic and electric properties. However, an experimental investigation of the magnetic structure evolution and its intimate relation

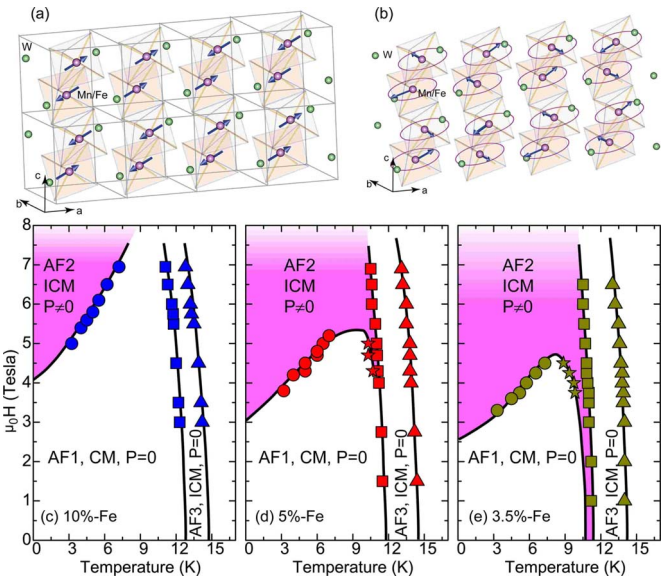

FIG. 1. (Color online) (a) Crystal and magnetic structures of $Mn_{1-x}Fe_xWO_4$ in the collinear commensurate phase at low T/H region. The magnetic spins lie in the ac plane with the moment canted to the a axis about 40° (Ref. 21). (b) The magnetic structure in the noncollinear incommensurate phase at high magnetic field. [(c)–(e)] The H/T phase diagram at $x=0.10$, 0.05, and 0.035.

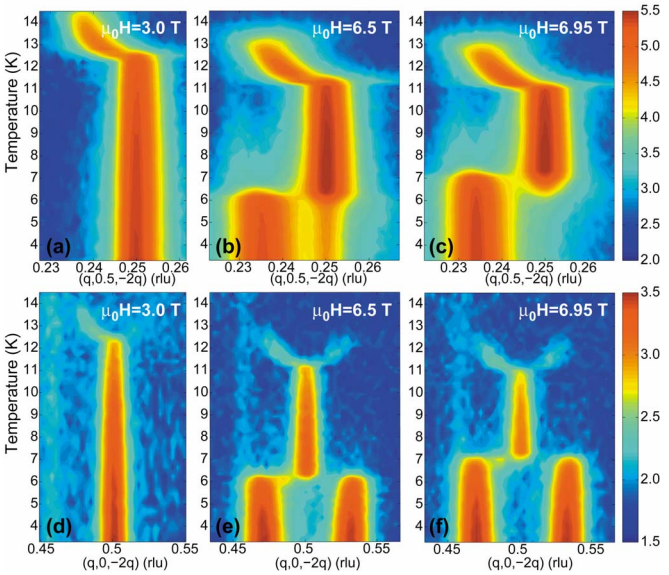

FIG. 2. (Color online) The temperature dependence of the magnetic [panels (a)–(c)] and structural [panels (d)–(f)] orders in $Mn_{0.90}Fe_{0.10}WO_4$ at fields of $\mu_0 H=3.0$, 6.5, and 6.95 T. All measurements are done upon warming after the sample is cooled to base temperature in the desired field.

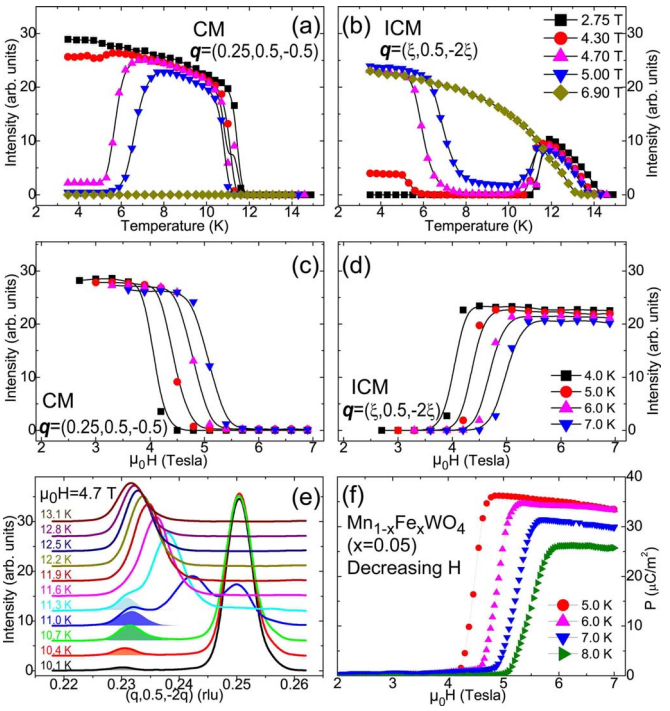

FIG. 3. (Color online) Magnetic and electric properties of $Mn_{0.95}Fe_{0.05}WO_4$ ($x=0.05$). The T dependence of the integrated intensities of (a) the CM and (b) the ICM magnetic peaks at selective fields. (c) and (d) show the field dependence of integrated intensities of the CM/ICM peaks at different temperatures. The sample is field cooled to the desired temperature and the measurements are carried upon lowering the field. (e) The wave vector scans near the transition at $\mu_0 H=4.7$ T. Shadow areas are the Gaussian fits to the ICM peak. (f) The field dependence of polarization (P) at different temperatures.

with the multiferroic property induced by both doping and magnetic field is still lacking. In this Brief Report, we report high-resolution elastic neutron-scattering measurements of the magnetic correlations in multiferroic $Mn_{1-x}Fe_xWO_4$ single crystals. We observed a systematic evolution of the phase diagram with increasing Fe doping. Under zero magnetic field, the noncollinear incommensurate (AF2) phase shrinks with increasing Fe concentration and disappears completely before $x=0.10$. This phase is recovered with magnetic field applied along the spin easy axis. Our results demonstrate that the exotic magnetic structure results from the delicate balance between competing magnetic interactions and are highly sensitive to small internal and external perturbations.

Single crystals of $Mn_{1-x}Fe_xWO_4$ ($x=0.035$, 0.05, 0.10, mass=3–5 g) were grown in an image furnace. The neutron-scattering measurements were performed at the HB1A three axis spectrometer at the Oak Ridge National Laboratory and BT9 spectrometer at the NIST Center for Neutron Research. A closed-cycle refrigerator in combination with a 7 T vertical field cryomagnet was used to achieve the desired temperature and field. The crystals were aligned in the scattering plane defined by the two orthogonal wave vectors (1,0,−2) and (0,1,0), in which the magnetic Bragg peaks and other structural peaks can be surveyed. The incident neutron energy was fixed at 14.7 meV using pyrolytic graphite crystals as monochromator, analyzer, and filter.

Figures 2(a)–2(c) show the temperature dependence of the magnetic scattering peaks in $Mn_{0.90}Fe_{0.10}WO_4$ at several magnetic fields. At $\mu_0 H=3$ T, only the CM magnetic peak $[q_{CM}=(0.25,0.5,-0.5)]$ exists at low temperatures. The peak intensities gradually decrease upon warming toward $T_{N1} \approx 12.4$ K. Above T_{N1}, the magnetic peak moves abruptly to the ICM position $q_{ICM}=(\xi,0.5,-2\xi)$, with ξ ranging from 0.235 to 0.25.[22] This is in sharp contrast with pure $MnWO_4$, where the noncollinear ICM magnetic phase is present for $7<T<12$ K. The ICM phase in the doped system is observed when the magnetic field increases. For $\mu_0 H=6.5$ T, the ICM magnetic peaks dominate at low T with remnant CM scattering indicative of phase competition. For a higher field of 6.95 T, the system exhibits only the long-range ICM magnetic order at low T. The H/T-phase diagram is constructed by identifying the corresponding transitions, as summarized in Fig. 1(c). The magnetic-field induced structural transitions are displayed in Figs. 2(d)–2(f). The superlattice peaks caused by the structural distortion closely track the magnetic order. Our observations are similar to the strong spin-lattice coupling observed in other multiferroic materials[23,24] and consistent with the result reported in pure $MnWO_4$.[25]

The modification of the phase diagram at lower Fe doping is exemplified by studying the T and H dependences of the magnetic orders in $Mn_{0.95}Fe_{0.05}WO_4$. Figures 3(a) and 3(b) display the thermal evolution of the integrated intensities of the CM and ICM phases at several magnetic fields, respectively. At low magnetic fields ($\mu_0 H<3$ T), the ICM phase is restricted to the high-T collinear order between 11 and 14 K. At low T, only the CM phase exists and there is no trace of the ICM magnetic state. For 3 T$<\mu_0 H<5$ T, the system

displays a coexistence of both phases. The spectral weight of the CM magnetic scattering shifts gradually to the ICM one at higher fields. For $\mu_0 H > 5$ T, the low-T phase is entirely ICM and ferroelectric. We have also studied the H dependence of the magnetic scattering, as shown in Figs. 3(c) and 3(d). The low-T ICM phase stabilized under field cooling (FC) changes abruptly into the CM phase when the magnetic field is lowered. Consistent with the T-dependent measurements, the critical magnetic field required for the ICM-CM transition decreases as the measured temperature lowers. For comparison, the electric polarization measurement under field lowering at similar temperatures is plotted in Fig. 3(f). The observed correlation between the ICM magnetic scattering and P highlights the intimate interplay between the magnetic and the electric properties.

Most interestingly, the $x=0.05$ sample exhibits a reentrant behavior (the disappearance and reappearance of the low-T ICM phase) in a narrow range of magnetic fields ($4\ \text{T} < \mu_0 H < 5\ \text{T}$) just below the CM/ICM transition. In Fig. 3(e), we show a series of wave vector scans across both the ICM and CM magnetic Bragg peaks as the sample is warmed at $\mu_0 H = 4.7$ T. Although the low-T scattering profile is dominated by the CM scattering peaks at $(0.25, 0.5, -0.5)$, the emergence of an ICM magnetic peak is clearly seen at 10.1 K at the wave vector $q_{\text{ICM}} = (0.23, 0.5, -0.46)$. The intensity initially grows with T, reaches a maximum at 10.7 K, and is suppressed upon further warming. The wave vector shows little temperature variation. At higher T's, the magnetic scattering evolves into the collinear ICM phase, where the peak position shows a strong temperature dependence.

The reentrant ferroelectric behavior is more evident at $x = 0.035$. Figure 4(a) displays the T dependence of the integrated intensities for this sample extracted from the ICM magnetic peak at several H's. At $\mu_0 H = 3.75$ T, the low-T ICM intensity collapses suddenly near 5 K, accompanying the enhancement of the CM peak (data not shown). Such a transition between the competing magnetic phases is similar to the low-field data at $x=0.05$. However, the ICM intensity starts to increase again as T just crosses 9 K, which is about 2 K lower than the expected AF2/AF3 phase boundary. The latter increase in the ICM intensity is accompanied by the reappearance of the FE polarization [Fig. 4(b)] suggesting that the ICM magnetic state between 9 and 12 K is the same as the low-T noncollinear electrical polar phase.

Unlike the case of higher Fe doping where the boundary of the paraelectric phase is well defined, the transition from low-T ICM phase to the high-T ICM phase becomes less discernible at $x=0.035$. To better characterize the phase boundary, we tracked the thermal evolution of the ICM peak position at different fields with higher resolution [Fig. 4(c)]. Although the temperature shift is much smaller compared to those presented in Figs. 2(a)–2(f) and 3(e), the boundaries at individual AF1/AF3 transitions are visible despite the lack of an anomaly in intensity [Fig. 4(a)]. In addition, the wave vector shows a distinct variation when the system re-enters the FE/ICM phase. The boundaries obtained from neutron scattering are in agreement with the polarization data in Fig. 4(b). Finally, we estimate the volume percentage $V_P(\%)$ of the polar state [Fig. 4(d)]. This is done by calculating $V_P(\%) = I_{\text{ICM}}/(I_{\text{ICM}} + I_{\text{CM}})$, where I_{ICM} and I_{CM} are the integrated ICM/CM intensities. Although there is considerable nonpolarized volume fraction at lower H/T regime, the fraction of the FE phase increases quickly with field and becomes saturated at $\mu_0 H = 4$ T. We further notice that the magnetic fluctuations below 12 K are mainly incommensurate, but the CM spin order gradually builds up at lower temperatures.

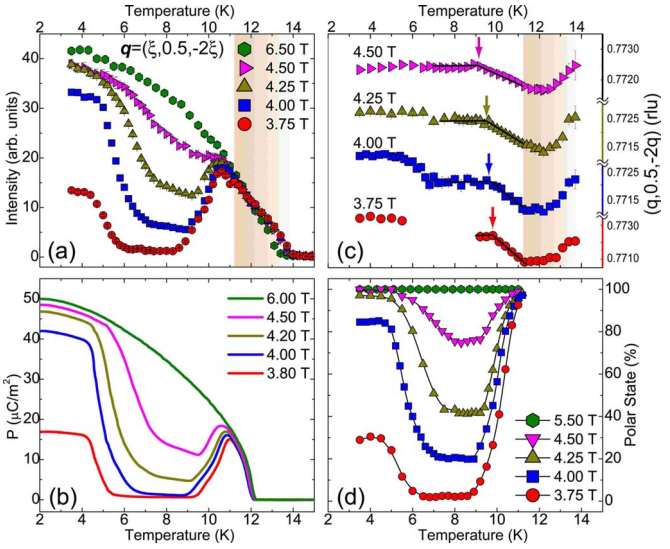

FIG. 4. (Color online) Magnetic and electric properties of $Mn_{0.965}Fe_{0.035}WO_4$ ($x=0.035$). (a) T dependence of the ICM magnetic peaks at different magnetic fields. (b) The polarization measurements under the same thermal protocol. (c) The evolution of the ICM wave vectors in selective magnetic fields. The arrows mark the transition where the system re-enters the ferroelectric phase. (d) The T dependence of the polar state volume fraction at different fields. Uncertainties in the plots are statistical and represent one standard deviation.

It is known that the magnetic properties of frustrated spin systems are sensitive to impurities and external stimuli. In contrast to the geometrically frustrated antiferromagnet $CuFeO_2$ where a 1.2% Al doping at the Fe site stabilizes the multiferroic phase,[26] the substitution of Mn by Fe in $MnWO_4$ suppresses such phase. The electric polar state observed in a moderate temperature range at $x=0$ is completely absent at $x=0.10$. Instead of forming an E-type spin order with zigzag AF chains along the c axis in $MnWO_4$, pure $FeWO_4$ has a relatively simple magnetic structure with magnetic wave vector $q_M = (0.5, 0, 0)$.[27] Previous inelastic neutron-scattering (INS) studies on $MnWO_4$ reported that the spin-wave dispersion relations can only be described by including magnetic coupling up to ninth nearest neighbors.[28] The INS data demonstrate that the stabilization of the CM spin order requires long-range magnetic interactions. It is expected that the substitution leads to modifications of the local environment around the magnetic ions, which ultimately causes a redistribution of exchange coupling strengths. On the other hand, despite the complex interactions associated with the crystal structure, Chaudhury *et al.*[20] proposed a simple mean-field model, including nearest- and next-nearest-neighbor interactions, spin anisotropy (K), and external magnetic field, to explain the observed phase diagram in Fe-doped $MnWO_4$. It

was speculated that the lack of ferroelectricity (at $H=0$) in $Mn_{0.9}W_{0.1}WO_4$ is due to the increase in the uniaxial anisotropy K. Based on a pressure-dependent study on $MnWO_4$,[29] which showed a pressure-induced suppression of the FE phase, the Fe doping can be viewed as an internal (chemical) pressure effect on the structure. Indeed, a noticeable decrease in Mn-O bonding distance within the edge-sharing octahedron is observed in the neutron powder refinement for the $x=0.10$ sample.

In summary, our neutron-scattering studies reveal a systematic evolution of magnetic properties in the multiferroic $Mn_{1-x}Fe_xWO_4$. The ICM spin structure associated with the FE phase at $H=0$ shrinks with increasing Fe concentration. The noncollinear magnetic configuration in the doped system is restored with the application of external magnetic field. Those results indicate that the complex spin structure accompanying spontaneous electric polarization results from competing magnetic interactions and is subject to both internal (chemical doping) and external (magnetic-field) perturbations.

We are grateful to R. S. Fishman and T. Kimura for helpful discussions. This work was partially supported by Division of Scientific User Facilities of the Office of Basic Energy Sciences, U.S. Department of Energy. This work utilized facilities supported in part by the National Science Foundation under Agreement No. DMR-0454672. Work at Houston was supported by the T.L.L. Temple Foundation, the J.J. and R. Moores Endowment, the U.S. Air Force Office of Scientific Research, and the State of Texas through TCSUH.

*yef1@ornl.gov

[1] S.-W. Cheong and M. Mostovoy, Nature Mater. **6**, 13 (2007).
[2] Y. Tokura, Science **312**, 1481 (2006).
[3] W. Eerenstein, N. D. Mathur, and J. F. Scott, Nature (London) **442**, 759 (2006).
[4] D. I. Khomskii, J. Magn. Magn. Mater. **306**, 1 (2006).
[5] T. Kimura, T. Goto, H. Shintani, T. Arima, and Y. Tokura, Nature (London) **426**, 55 (2003).
[6] T. Goto, T. Kimura, G. Lawes, A. P. Ramirez, and Y. Tokura, Phys. Rev. Lett. **92**, 257201 (2004).
[7] N. Hur, S. Park, P. A. Shama, J. S. Ahn, S. Guha, and S.-W. Cheong, Nature (London) **429**, 392 (2004).
[8] G. Lawes, A. B. Harris, T. Kimura, N. Rogado, R. J. Cava, A. Aharony, O. Entin-Wohlman, T. Yildrim, M. Kenzelmann, C. Broholm, and A. P. Ramirez, Phys. Rev. Lett. **95**, 087205 (2005).
[9] N. Ikeda, H. Ohsumi, K. Ohwada, K. Ishii, T. Inami, K. Kakurai, Y. Murakami, K. Yoshii, S. Mori, Y. Horibe, and H. Kitô, Nature (London) **436**, 1136 (2005).
[10] T. Kimura, J. C. Lashley, and A. P. Ramirez, Phys. Rev. B **73**, 220401(R) (2006).
[11] Y. Yamasaki, H. Sagayama, T. Goto, M. Matsuura, K. Hirota, T. Arima, and Y. Tokura, Phys. Rev. Lett. **98**, 147204 (2007).
[12] H. Katsura, N. Nagaosa, and A. V. Balatsky, Phys. Rev. Lett. **95**, 057205 (2005).
[13] I. A. Sergienko and E. Dagotto, Phys. Rev. B **73**, 094434 (2006).
[14] M. Mostovoy, Phys. Rev. Lett. **96**, 067601 (2006).
[15] K. Taniguchi, N. Abe, T. Takenobu, Y. Iwasa, and T. Arima, Phys. Rev. Lett. **97**, 097203 (2006).
[16] O. Heyer, N. Hollmann, I. Klassen, S. Jodlauk, L. Bohatý, P. Becher, J. A. Mydosh, T. Lorenz, and D. Khomskii, J. Phys.: Condens. Matter **18**, L471 (2006).
[17] A. H. Arkenbout, T. T. M. Palstra, T. Siegrist, and T. Kimura, Phys. Rev. B **74**, 184431 (2006).
[18] O. Prokhnenko, R. Feyerherm, E. Dudzik, S. Landsgesell, N. Aliouane, L. C. Chapon, and D. N. Argyriou, Phys. Rev. Lett. **98**, 057206 (2007); O. Prokhnenko, R. Feyerherm, M. Mostovoy, N. Aliouane, E. Dudzik, A. U. B. Wolter, A. Maljuk, and D. N. Argyriou, *ibid.* **99**, 177206 (2007).
[19] G. Lautenschläger, H. Weitzel, T. Vogt, R. Hock, A. Böhm, M. Bonnet, and H. Fuess, Phys. Rev. B **48**, 6087 (1993); H. Ehrenberg, H. Weitzel, C. Heid, H. Fuess, G. Wltschek, T. Kroener, J. van Tol, and M. Bonnet, J. Phys.: Condens. Matter **9**, 3189 (1997).
[20] R. P. Chaudhury, B. Lorenz, Y. Q. Wang, Y. Y. Sun, and C. W. Chu, Phys. Rev. B **77**, 104406 (2008).
[21] High resolution neutron powder-diffraction measurements confirm that the low-T magnetic structure of $x=0.10$ sample at AF1 phase is the same as the pure $MnWO_4$.
[22] Although the actual wave vector associated with the ICM magnetic peak is $(h,k,l)=(0.234,0.5,-0.46)$, the current scattering configuration still allows us to probe the ICM peak due to the coarse vertical resolution of the spectrometer.
[23] L. C. Chapon, G. R. Blake, M. J. Gutmann, S. Park, N. Hur, P. G. Radaelli, and S.-W. Cheong, Phys. Rev. Lett. **93**, 177402 (2004).
[24] F. Ye, Y. Ren, Q. Huang, J. A. Fernandez-Baca, Pengcheng Dai, J. W. Lynn, and T. Kimura, Phys. Rev. B **73**, 220404(R) (2006).
[25] K. Taniguchi, N. Abe, H. Sagayama, S. Otani, T. Takenobu, Y. Iwasa, and T. Arima, Phys. Rev. B **77**, 064408 (2008).
[26] S. Kanetsuki, S. Mitsuda, T. Nakajima, D. Anazawa, H. A. Katori, and K. Prokes, J. Phys.: Condens. Matter **19**, 145244 (2007).
[27] N. Stüßer, Y. Ding, M. Hofmann, M. Reehuis, B. Ouladdiaf, G. Ehlers, D. Günther, M. Meißner, and M. Steiner, J. Phys.: Condens. Matter **13**, 2753 (2001).
[28] H. Ehrenberg, H. Weitzel, H. Fuess, and B. Hennion, J. Phys.: Condens. Matter **11**, 2649 (1999).
[29] R. P. Chaudhury, F. Yen, C. R. dela Cruz, B. Lorenz, Y. Q. Wang, Y. Y. Sun, and C. W. Chu, Physica B (Amsterdam) **403**, 1428 (2007).